

Forced Convective Heat Transfer Effects and Flow Resistance in a Packed Bed Column with Al₂O₃ Nano Fluid

G. Srinivasrao^{a*}, K.V. Sharma^b, S.P. Chary^c, M.T. Naik^d

^aDepartment of Mechanical Engineering, Kakatiya Institute of Technology and Science, Warangal-506015, India

^bFaculty of Mechanical Engineering, Universiti Malaysia Pahang, 26600 Pekan, Pahang, Malaysia

^cRetd. Professor, Andhra University, Visakhapatnam-530045, India

^dFaculty of center for Energy, JNTUH, Hyderabad

Received 25 Nov. 2011; accepted 30 Nov.2011, Available online 1 Dec. 2011

Abstract

This study explores the pressure drop, friction coefficient, flow resistance factor and forced convective Heat transfer effects in a packed bed column with two different diameter glass beds D_p (6mm,14.56mm) with the packed bed Reynolds number ($Re_p=500$ to 1500). Al₂O₃ nano fluid introduced in the experimental testrig in three different concentrations 0.02%, 0.1%, and 0.5% respectively against the gravity. The results indicate that resistance approaches a minimum in higher diameter particle and minimum concentration of Al₂O₃. The influence of volume concentration percentage of nano particles on the friction factor, pressure drop, and convective heat transfer can achieve a higher average Nusselt number value for its higher concentration. Therefore, three dominated parameters (ϵ , Re_p , ϕ) need to be compromised for their effects in the above mentioned C_f and N_u . The proposed empirical correlation equations of friction factor (f), Nusselt number (N_u) with volume concentration and particle diameter are $f = 20.0593 Re_p^{-0.3117} (1 + \phi)^{0.2919}$ and $Nu = 0.188 Re_p^{0.98} (1 + \phi)^{0.5310} Pr^{-0.4403}$

Keywords: Packed bed, Nanofluid, Convective heat transfer, Friction factor, Nusselt number

1. Introduction

Porous media are extensively adopted in many applications, such as the domain ranges from catalytically and chemical particle beds, mass separator units and heat exchangers to thermal insulation, debris bed, soil investigations (oil recovery), heat pipes and fluidized beds. Achenbach [1] experimentally presented the heat transfer and flow characteristics of packed beds, and proposed equations for predicting the convective heat transfer, pressure drop, effective thermal conductivity and wall heat transfer. The flow resistance and forced convective heat transfer is both necessary and critical studies, with the former dominating the viscous interaction, energy loss and the resulting pressure drop, and the latter determining the heat removal and the corresponding Nusselt number. Many early works concentrated on resistance and heat transfer. Ergun [2] discussed the fluid flow through packed columns, and proposed treating the total energy loss in fixed beds as the sum of the adhesive and kinetic energy losses. A new form of resistance factor, Nu, represent the proportion of

pressure drop to the viscous energy term. Kuo and Nydegger [3] finished flow resistance measurement and correlation in a packed bed of WC870 ball propellants, proposing a relationship that extends the highest Reynolds number range of Ergun's correlation [2] by a factor of 10. Jones and Krier [4] demonstrated that the classical Reynolds number dependence of the coefficient of drag for gases forced into packed beds is not true at high Reynolds numbers, and proposed that the Ergun correlation [2] cannot extend beyond Reynolds numbers of 10^3 . Foumeny et al. [5] examined the pressure-drop characteristics of beds of equilateral and non-equilateral solid cylinders of aspect ranging from 0.5 to 2.0. An empirical correlation to predict pressure drop in beds of cylindrical particles has also been developed. The boundary and inertia effects on convective flow and heat transfer were analyzed by Vafai and Tien [6] for constant porosity media and expressed in terms of different governing parameters. These effects were also investigated by an experiment [7] for transient mass transfer through uniform porous media. The variable porosity on flow and heat transfer in variable porosity media was also performed through an experimental and

* Corresponding Author E-mail: gsrkits@gmail.com

numerical analysis [8]. Energy transport capacity of a nanofluid is affected by the quality and dimensions of the nano-particles as well as the volume fraction.

Experimental investigations have revealed that nano fluids have higher values of thermal conductivity than those of the pure liquids and greater potential for heat transfer enhancement [9-11]. Compared with the existing techniques for enhancing heat transfer, nano fluids are ideally suited for practical applications incurring little or no difficulty in pressure drop because of their size and as such 'behaves' like a pure fluid under flow conditions.

Mansour et al. [12] studied the effect of uncertainties in nanofluid thermo physical properties and stated that the evaluation of heat transfer rate depends on the accuracy with which the properties are evaluated. Thermal conductivity of water- γ -Al₂O₃ nanofluid has been evaluated experimentally by Das et al. [13] in the temperature range of 21-51°C and observed 2 to 4 fold enhancements in the range of concentration tested. Wen and Ding [14] conducted experiments with water + Al₂O₃ nanofluid to calculate heat transfer rates in the entrance area under laminar flow conditions. They used equations present in studies to determine viscosity at bulk temperatures. They showed that Shah equation [8] related to real liquids failed to predict the heat transfer behavior under similar flow conditions with nanofluids. Maiga et al. [15] investigated the water- Al₂O₃ and Ethylene glycol, Al₂O₃ nanofluids and observed adverse effects of wall shear when tested with the later. Pak and Cho [16] performed experiments for the evaluation of turbulent friction and heat transfer behavior of γ -Al₂O₃ and TiO₂ dispersed in water. The results showed that Nusselt number of the dispersed fluid increase with increasing volume fraction of the suspended solid particles and the Reynolds number. Lee and Choi [17] used nanofluid as a coolant in a micro channel heat exchanger for cooling crystal silicon mirrors used in high intensity X-ray sources and pointed out that nanofluid shown better cooling rates when compared with water or liquid nitrogen cooled micro channel heat exchangers. Xuan, Y., and Roetzel, W., [18] studied about the correlation in nano fluids. P.K.Sarma, T.Subramanyam, P.S.Kishore, V.Dharma Rao [19] handle the some experiments in laminar flow with Convective Heat Transfer with Twisted Tape Inserts in a tube. K.V.Sharma L. Syam Sundar and S. Ramanathan[20] investigates the enhancement of heat transfer coefficient with twisted tape insert in a Circular Tube with Al₂O₃ nano fluids in different volume concentrations. The reasons of heat transfer enhancement of the nanofluids may be required to intensification of turbulence or eddy, suppression of the boundary layer as well as dispersion or before mixing of the suspended nanoparticles, a large enhancement in the surface area of nanoparticles, besides substantial augmentation of the thermal conductivity and the heat capacity of the fluid. Therefore, the convective

heat transfer coefficient with nanofluid can be a function of the physical properties of the constituents, capacity and volume fraction of suspended nanoparticles as well as the flow velocity.

The above mentioned investigations focused on flow resistance and convective heat transfer, but did not consider the effects of nano fluids and its volume concentration. The present work is aimed at establish single phase heat transfer coefficients with water and water based Al₂O₃ nanofluid in a tube with packed materials of glass beds under different flow conditions.

Therefore, this paper experimentally investigates the effects of three types volume concentration of Al₂O₃ nanofluid on flow resistance and forced convective heat transfer, and compares the effect of porosity and hydraulic Reynolds number. This research also establishes a series of feasible correlation equations for three flow volume concentration of nano fluids, which can be followed to obtain appropriate practical application parameters.

2. Parametric definitions

The void fraction (porosity, ε) is defined as

$$\varepsilon = \frac{v_t - v_s}{v_t} \quad (1)$$

Where v_s and v_t represent the solid volume and total volume, respectively. Du Plessis and Woudberg (2008) define as particle Reynolds number as

$$Re_p = \frac{\rho_f V_0 D_p}{\mu_f} = \frac{\rho_f \varepsilon V_{av} D_p}{\mu_f} \quad (2)$$

Where ρ_f is the fluid density μ_f the fluid viscosity and V_{av} is the average interfacial velocity (fluid velocity in the pores between particles) and at cross –section in the bed. It is related to the superficial velocity V_0 by the relationship

$$V_0 = \varepsilon V_{av} \quad (3)$$

D_p is the hydraulic diameter of the particle, while V_0 is the superficial velocity of the fluid passing through the porous packed bed media. Most works including Bennett and Myers (1962), Diedericks (1999), Du Plessis (2002) and Martin (2005) spend this superficial velocity, defined as

$$V_0 = \frac{m_f}{\rho_f A_{cs}} \quad (4)$$

Uses slightly different definitions, a partial derivation of which is provided by Bennett and Myers (1962). The Ergun Reynolds number (Ergun, 1952) includes a void fraction dependent term

$$\frac{Re_{er} = \rho_f V_0 D_p}{\mu_f (1-\varepsilon)} \quad (5)$$

The hydraulic diameter of the pore size between particles may be estimated from an equation given by Diedericks (1999)

$$D_h = 4R_h = \frac{4\varepsilon v_t}{A_s} = \frac{4\varepsilon}{A_{vs}(1-\varepsilon)} \tag{6}$$

R_h is the hydraulic radius of the pore, defined as the ratio of cross-section available for flow to wetted perimeter, or alternatively, volume available for flow to total wetted surface. In variable from,

$$R_h = \frac{\frac{v_f}{v_t}}{\frac{A_s}{A_{vs}}}$$

for a cube, the total solid surface area is $A_s = 6D_p^2$. The constant volume specific surface area $A_{vs} = A_s/v_t(1-\varepsilon) = 6/D_p$. The table 1 represents the operating parameters of the experimental setup.

3. Fabrication of the experimental setup

The experimental setup consists of 0.04 m dia., 0.5 m

height of a packed bed column. A 50 liters feed water storage tank, a heating tank for regulating inlet water temperature and a one HP pump for circulating water are other accessories. Flow control valve and bypass valve are incorporated in the track for regulating the flow rate. Rotometer, manometer and thermocouples are connected in the circuit for measurement of flow, pressure drop and temperatures respectively. All the thermocouples are connected to the data logger and it is connected to the personnel computer for recording and storing the data. The methodology and instrumentation diagram of the experimental set up is shown in figure 1. From the storage tank the fluid is pumped with the help of a pump into a helical coil which is immersed in the heating tank. The water in the heating tank is heated with immersion heater. The pumping fluid is heated with this hot water upto the required temperature before it enters the test section. The interaction between cold bed and this hot fluid takes place, as a result the fluid temperature at bed outlet decreases. This fluid is re-circulated in a closed circuit. After the bed reaches the steady state temperature pressure drop across the bed and temperatures along the bed axial length are noted with the help of a data logger and the data is stored in personal computer. The experimental data are obtained for two different glass bead dia. of sizes 6 mm and 14.6 mm

Table 1 Operating parameters

Flow rate	Particle diameter	Porosity	Fluid inlet temperature	Reynolds number
150LPH to 300LPH	6mm, 14.56mm	0.49, 0.389	40°C to 55°C	500 to 1500



Fig 1 Experimental test rig setup

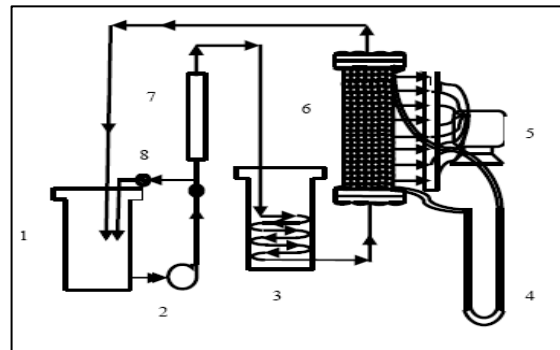


Fig 2.0 schematic diagram of experimental setup

- 1. Supply tank 2. Pump 3. Heating tank with heating element
- 4. Manometer 5. PC with data logger 6. test section 7. Rotameter
- 8. Back flow

Table 2 Correlations

Fluid	Water		Al203Nano fluid		Al203Nano fluid		Al203Nano fluid 0.02%	
	a1	b1	a1	b1	a1	b1	a1	b1
14.56mm	281.72	2.065	288.72	2.065	298.53	2.135	305.9	2.1875
6mm	180.012	2.1	179.011	2.1	179.99.00	2.1	180	2.1

4. Results and discussion

Fig. 3 shows the friction coefficient C_f versus $Re_p/(1-\varepsilon)$ under different fluid flow conditions for water and nano fluids and different diameters of D_p . The value of C_f was calculated by applying

$$f = \frac{\Delta P_{Exp}}{L_B} \frac{D_p}{\rho V_s^2} \frac{\varepsilon^3}{1 - \varepsilon} \quad (7)$$

presented by Jones and Krier [4]. To correlate the relationship among f , Re_p and flow resistance factor F_v is defined as

$$F_v = f / Re_p (1 - \varepsilon) \quad (8)$$

Ergun [2] previously proposed another equation

$$F_v = 150 + 1.75 \frac{Re_d}{(1 - \varepsilon)} \quad (9)$$

From the least square fit the followed Regression equation is

$$F_v = a + b \frac{Re_d}{(1 - \varepsilon)} \quad (10)$$

From the experimental results the proposed relationship for water and Al_2O_3 nano fluid is as follows. For 14.56mm particle the different proposed correlation are represented in table 2.

5. Results and discussions

The pressure drop, friction factor and the Nusselt number distribution for different experimental parameters for water and nano fluid with different concentrations is presented with Fig. 3 to 6

Fig. 3 represents the pressure drop in the packed bed with water and nano fluids at different volumetric concentrations. The pressure drop increase with particle diameter and particle Reynolds number. The pressure drop in the case of nano fluids increases with volume concentration. Fig 4 represents a comparison of experimental and theoretical friction factor for water and nano fluid at different concentrations for both 6mm and 14.56mm particles. The friction factor increases with lowering particle diameters and increasing concentration of the nanofluid.

Fig. 5 & 6 present the form of heat transfer coefficient for different concentrations of nano fluid. Fig 5 shows the variation of heat transfer coefficient with particle Reynolds. Nanofluid predicts higher heat transfer coefficients compared to base fluid water.

The results from the three volume concentration vary considerably. The convection effects then decay along the flow axis, causing the temperature distributions to increase linearly with the decreases in X/L . Because of the fluid flow concentration, thus causing a linear decay in the temperature distributions and the corresponding

convection in a high-temperature sector is worse than that in a low-temperature zone. Therefore, a convection stagnation area exists at the peak location. With respect to porosity effects, a smaller D_p was found to result in a larger surface area for convective heat transfer, yielding a lower overall temperature graph. The temperature difference between D_p of 6 mm and D_p of 14.56 mm is almost up to $2^{\circ}C$ to $5^{\circ}C$. The variation of Nu is dominated for different volume concentration of and fluid inlet temperature. Therefore, the Nusselt number was found to be highest for the higher concentration fluid due to because of the good convection heat transfer in fluid. The Nu distributions varied sharply for the 6mm particle than 14.56mm particle due to increases in the large surface area and number of particles.

The following discussion focuses on the effect of particle Reynolds number (Re_p), as illustrated in as Re_p decreases there is increases, intensifying the forced convection effects enhances the convective heat transfer. To understand the relationships of the average Nusselt number versus the packed bed Reynolds number, all of the relational measured data must be estimated, resulting in a series of practical correlation equations. The results in Fig. 6 reveal that the overall average Nusselt number is presented according to least square fit is for 14.56mm, 6mm particles. The equation (12) represents the correlation results for Nusselt number and Reynolds number and volume concentration of nano fluid.

6. Conclusions

This work experimentally investigated the flow resistance and forced convective heat transfer standing for three types of volume concentrations in a vertical packed bed column. The other parameters include the glass beds diameter (porosity) and the packed bed Reynolds number. The results reveal that the friction factor and flow resistance parameter is lowest for the higher volume concentration and higher in the water due to the variation in the Reynolds number. Conversely, the effect of flow concentration on convective heat transfer is irrelevant, with increasing in the volume concentration of Al_2O_3 exhibiting higher average Nusselt number value. As expected, the increase of porosity and particle packed bed Reynolds number augmented both the flow resistance and the convective heat transfer, and the two dominated parameters (ε , Re_p) need to compromised for their positive/negative effects in the above mentioned. Therefore, this study presents an empirical correlation equation of Nu vs. Re_p for the different volume concentrations of Al_2O_3 , 6 mm and 14.56 mm diameter glass beds to provide a fast and effective framework in specifying appropriate parameters for different relational

practical applications. A regression equation is obtained for the estimation of friction factor with an average deviation of $\pm 0.08\%$ and standard deviation of 1.68%

$$f = 20.0593 Re_p^{-0.3117} (1 + \phi)^{0.2919} \tag{11}$$

A regression equation is developed for the estimation of Nusselt number as a function of particle Reynolds number, Prandtl and volume concentration of nanofluid. It is obtained with a standard deviation of 1.56% and an standard deviation of -3.92% given by

$$Nu = 0.188 Re_p^{0.98} (1 + \phi)^{0.5310} Pr^{-0.4403} \tag{12}$$

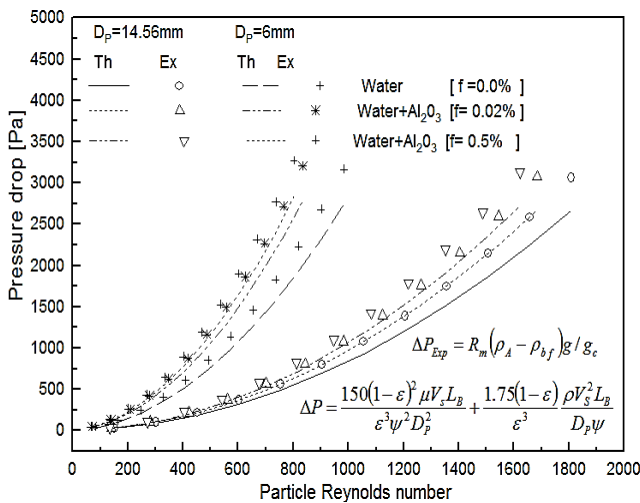


Fig 3 Pressure drop V/s Particle Reynolds number for water and Al₂O₃ nano fluid

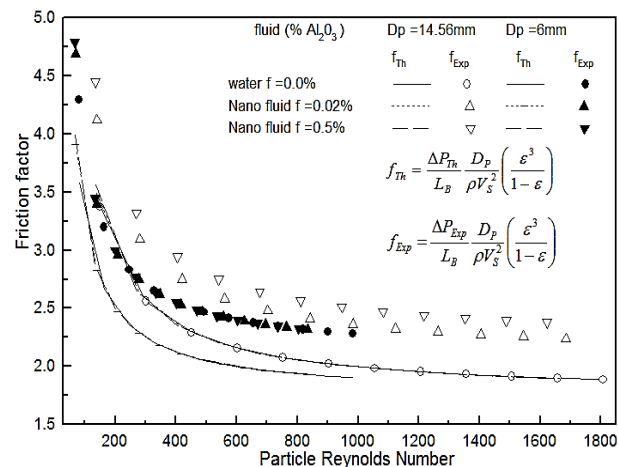


Fig 4 Friction factor V/s Particle Reynolds number for Water and nano fluid

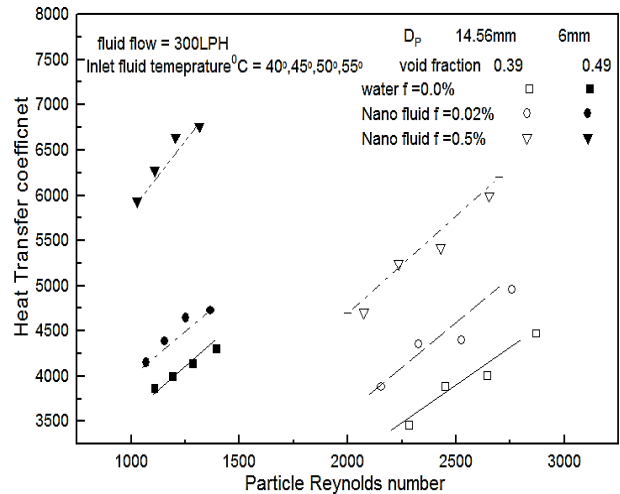


Fig 5 Heat transfer coefficient V/s particle Reynolds number Reynolds number for high flow rates

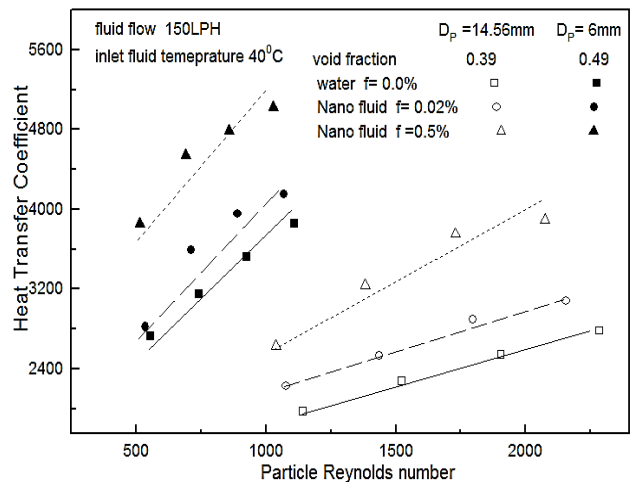


Fig 6 Comparison of Heat transfer coefficient V/s particle for high flow rates

References

1. E. Achenbach (1995), Heat and flow characteristics of packed beds, *Experimental Thermal and Fluid Science*, 10 pp.17-27.
2. S. Ergun (1952), Fluid flow through packed columns, *Chemical Engineering Progress*, 48 (2), pp. 89-94.
3. K.-K. Kuo, C.C. Nydeger (1978), Flow resistance measurement and correlation in a packed bed of WC 870 ball propellants, *Journal of Ballistics*, 2, pp. 1-25.
4. D.P. Jones, H. Krier (1983), Gas flow resistance measurements through packed bed at high Reynolds numbers, *Transaction of ASME Journal of Fluid Engineering*, 105, pp.168-173.
5. E.A. Foumeny, A. Kulkarni, S. Roshani, A. Vitani (1996), Elucidation of pressure drop in packed-bed systems, *Applied Thermal Engineering*, pp.195-202.
6. K. Vafai, C.L. Tien (1981), Boundary and inertia effects on flow and heat transfer in porous media, *International Journal of Heat and Mass Transfer*, 24, pp.195-203.

7. K. Vafai, C.L. Tien (1982), Boundary and inertia effects on convective mass transfer in porous media, *International Journal of Heat and Mass Transfer*, 25, pp.1183–1190.
8. K. Vafai, R.L. Alkire, C.L. Tien (1985), An experimental investigation of heat transfer in variable porosity media, *Transaction of ASME Journal of Heat Transfer*, 107, pp. 642–647.
9. Wang. X., Xu, X., and Choi, S.U.S. (1999), Thermal conductivity of nanoparticles fluid mixture, *J. Thermophys. Heat transfer*, 13(4), pp. 474- 480.
10. Lee, S., Choi, S.U.S., Li, S., and Eastman, J.A. (1999), Measuring thermal conductivity of fluids containing metallic oxide nanoparticles, *J. Heat transfer*, 121, pp. 280-289.
11. Li, Q., and Xuan, Y. (2000), Experimental investigation on transport properties of transfer with Nanofluids, *Applied Thermal Engineering*, 27, pp. 240-249.
12. Mansour, Nicolas Galanis, C.T.Nguyen (2007), Effect of uncertainties on forced convection heat nanofluids, Heat transfer science and technology, *Wang Buxuan, ed., Higher education press*, pp. 757-762.
13. Das.S.K, Nandy Putra, Peter Thiesen, Roetzel (2003), Temperature Dependence of Thermal Conductivity Enhancement for Nanofluids, *ASME Journal of Heat Transfer*, 125, pp. 567-574
14. Wen and Ding, (2004), Experimental Investigation into Convective Heat Transfer of Nanofluids at the Entrance Region under Laminar Flow Conditions, *IJHMT*, Vol.47, pp. 5181 5188.
15. Maiga, S.J.Palm, C.T.Nguyen, G.Roy, N.Galanis (2005), Heat Transfer Enhancement by Using Nanofluids in Forced Convection Flows, *IJHFF*, Vol.26, pp. 530-546.
16. Pak, B.C., and Cho, Y.I., (1998), Hydrodynamic and heat transfer study of dispersed fluids with submicron metallic oxide particles, *Exp. Heat transfer*, 11, pp. 151-170.
17. Lee, S., and S.U.S. Choi (1996), Application of metallic nanoparticles suspensions in advanced cooling systems, recent advance in solid/structures and application of metallic materials, L. Shinpho, Eds PVP, Vol 342/MD-vol. 72, ASME, New York, pp. 227-234.
18. Xuan, Y., and Roetzel, W.(2000), Conceptions for heat transfer correlation of nanofluids, *Int. J. Heat Mass Transfer.*, 43, pp. 3701-3707.
19. P.K.Sarma, T.Subramanyam, P.S.Kishore, V.Dharma Rao, Sadik Kakac (2003), Laminar Convective Heat Transfer with Twisted Tape Inserts in a Tube, *IJTS*, vol.42, pp. 821-828.
20. L. Syam Sundar, K.V.Sharma , S. Ramanathan (2007), Experimental investigation of Heat Transfer Enhancements with Al₂O₃ Nanofluid and Twisted Tape Insert in a Circular Tube, *International Journal of Nanotechnology and Applications*, Volume 1 Number 2 (2007) pp. 21–28.

Nomenclature

<i>a1, b1</i>	<i>constants</i>
<i>f</i>	<i>coefficient of friction</i>
<i>Fv</i>	<i>friction resistance</i>
<i>v</i>	<i>volume of column (m³)</i>
<i>Re</i>	<i>Hydraulic Reynolds number /Particle Reynolds number</i>
<i>V</i>	<i>superficial velocity (m/sec)</i>
<i>D</i>	<i>diameter (m)</i>
<i>m</i>	<i>mass flow rate(kg/sec)</i>
Greek symbols	
ρ	<i>density (Kg/m³)</i>
μ	<i>absolute viscosity (N-sec/m²)</i>
ϵ	<i>porosity</i>
<i>f</i>	<i>volume concentration of Al₂O₃Suffix</i>
<i>t</i>	<i>total</i>
<i>s</i>	<i>solid</i>